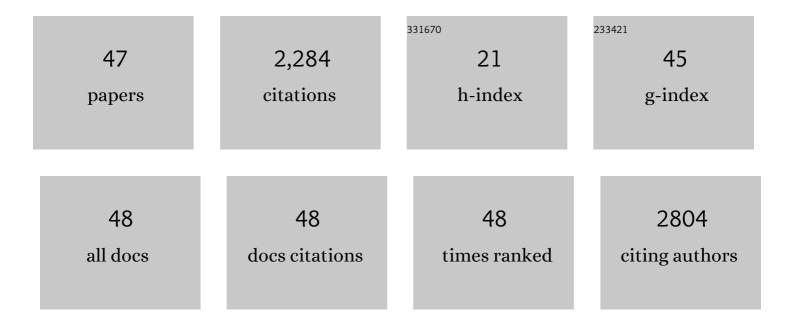
Marie-José Casanove

List of Publications by Year in descending order

Source: https://exaly.com/author-pdf/4904101/publications.pdf

Version: 2024-02-01



#	Article	IF	CITATIONS
1	Synthesis and Magnetic Properties of Nickel Nanorods. Nano Letters, 2001, 1, 565-568.	9.1	515
2	Ligand-Stabilized Ruthenium Nanoparticles:Â Synthesis, Organization, and Dynamics. Journal of the American Chemical Society, 2001, 123, 7584-7593.	13.7	336
3	Shape Control of Thermodynamically Stable Cobalt Nanorods through Organometallic Chemistry. Angewandte Chemie - International Edition, 2002, 41, 4286-4289.	13.8	335
4	Synthesis and Isolation of Cuboctahedral and Icosahedral Platinum Nanoparticles. Ligand-Dependent Structures. Chemistry of Materials, 1996, 8, 1978-1986.	6.7	148
5	A New Synthetic Method toward Bimetallic Ruthenium Platinum Nanoparticles; Composition Induced Structural Changes. Journal of Physical Chemistry B, 1999, 103, 10098-10101.	2.6	125
6	Quantitative analysis of HOLZ line splitting in CBED patterns of epitaxially strained layers. Ultramicroscopy, 2006, 106, 951-959.	1.9	81
7	Precursor Evolution and Nucleation Mechanism of YBa2Cu3Ox Films by TFA Metalâ^'Organic Decomposition. Chemistry of Materials, 2006, 18, 6211-6219.	6.7	58
8	Fully Crystalline Faceted Fe–Au Core–Shell Nanoparticles. Nano Letters, 2015, 15, 5075-5080.	9.1	55
9	Structure and chemical order in Co–Rh nanoparticles. Europhysics Letters, 2006, 73, 885-891.	2.0	44
10	Magnetic nanoparticles through organometallic synthesis: evolution of the magnetic properties from isolated nanoparticles to organised nanostructures. Faraday Discussions, 2004, 125, 265.	3.2	38
11	Inhomogeneous spatial distribution of the magnetic transition in an iron-rhodium thin film. Nature Communications, 2017, 8, 15703.	12.8	37
12	Segregation at a small scale: synthesis of core–shell bimetallic RuPt nanoparticles, characterization and solid state NMR studies. Journal of Materials Chemistry, 2012, 22, 3578.	6.7	34
13	Spontaneous Outcropping of Selfâ€Assembled Insulating Nanodots in Solutionâ€Đerived Metallic Ferromagnetic La _{0.7} Sr _{0.3} MnO ₃ Films. Advanced Functional Materials, 2009, 19, 2139-2146.	14.9	33
14	Structural and electronic properties of the Au(001)/Fe(001) interface from density functional theory calculations. Physical Review B, 2012, 86, .	3.2	32
15	Determination of precipitate strength in aluminium alloy 6056-T6 from transmission electron microscopy <i>in situ</i> straining data. Philosophical Magazine A: Physics of Condensed Matter, Structure, Defects and Mechanical Properties, 1997, 76, 921-931.	0.6	31
16	Growth and relaxation mechanisms in La0.66Sr0.33MnO3 manganites deposited on SrTiO3(0 0 1) and MgO(0 0 1). Applied Surface Science, 2002, 188, 19-23.	6.1	30
17	Interaction between solution derived BaZrO3 nanodot interfacial templates and YBa2Cu3O7 films leading to enhanced critical currents. Acta Materialia, 2011, 59, 2075-2082.	7.9	30
18	Towards MRI T2 contrast agents of increased efficiency. Journal of Magnetism and Magnetic Materials, 2015, 377, 348-353.	2.3	28

#	Article	IF	CITATIONS
19	Straining mechanisms in aluminium alloy 6056. In-situ investigation by transmission electron microscopy. Materials Science & Engineering A: Structural Materials: Properties, Microstructure and Processing, 2003, 340, 286-291.	5.6	27
20	Magnetic properties of Co _N Rh _M nanoparticles: experiment and theory. Faraday Discussions, 2008, 138, 181-192.	3.2	24
21	Structural, magnetic, transport, and magneto-optical properties of single crystal La2/3Sr1/3MnO3 thin films. Journal of Applied Physics, 2000, 87, 6773-6775.	2.5	22
22	The gold/ampicillin interface at the atomic scale. Nanoscale, 2015, 7, 14515-14524.	5.6	20
23	Epitaxial growth of magnetic Au/Co/Au sandwiches studied by TEM. Journal of Crystal Growth, 1997, 182, 394-402.	1.5	18
24	New approach for the dynamical simulation of CBED patterns in heavily strained specimens. Ultramicroscopy, 2008, 108, 426-432.	1.9	17
25	Chemical Solution Approaches to YBa ₂ Cu ₃ O _{7â~îî} -Au Nanocomposite Superconducting Thin Films. Journal of Nanoscience and Nanotechnology, 2011, 11, 3245-3255.	0.9	16
26	Noble Metal Nanocluster Formation in Epitaxial Perovskite Thin Films. ACS Omega, 2018, 3, 2169-2173.	3.5	15
27	How interface properties control the equilibrium shape of core–shell Fe–Au and Fe–Ag nanoparticles. Nanoscale, 2020, 12, 18079-18090.	5.6	15
28	On the Use of Amine–Borane Complexes To Synthesize Iron Nanoparticles. Chemistry - A European Journal, 2013, 19, 6021-6026.	3.3	10
29	Strain effects on the structural, magnetic, and thermodynamic properties of the Au(001)/Fe(001) interface from first principles. Physical Review B, 2014, 90, .	3.2	10
30	Evidence of a minority monoclinic LaNiO _{2.5} phase in lanthanum nickelate thin films. Physical Chemistry Chemical Physics, 2017, 19, 9137-9142.	2.8	10
31	Influence of a compositional gradient in the structure and magnetic behavior of strained FeMn ultrathin layers. Physical Review B, 1998, 58, 14135-14138.	3.2	9
32	Formation of Bimetallic FeBi Nanostructured Particles: Investigation of a Complex Growth Mechanism. Journal of Physical Chemistry C, 2013, 117, 1477-1484.	3.1	9
33	Study of the role of the ligands coordinated at the surface of pure Wüstite nanoparticles prepared following a room temperature organometallic method: Evidence of ferromagnetic – in shell- and antiferromagnetic – in core magnetic behaviors. Materials Chemistry and Physics, 2011, 129, 605-610.	4.0	8
34	Magnetism and morphology in faceted B2-ordered FeRh nanoparticles. Europhysics Letters, 2016, 116, 27006.	2.0	8
35	Role of the shell thickness in the core transformation of magnetic core(Fe)-shell(Au) nanoparticles. Physical Review Materials, 2019, 3, .	2.4	8
36	Effect of sample bending on diffracted intensities observed in CBED patterns of plan view strained samples. Ultramicroscopy, 2008, 108, 295-301.	1.9	7

MARIE-JOSé CASANOVE

#	Article	IF	CITATIONS
37	Strain induced atomic structure at the Ir-doped LaAlO ₃ /SrTiO ₃ interface. Physical Chemistry Chemical Physics, 2017, 19, 28676-28683.	2.8	7
38	Equilibrium shape of core(Fe)–shell(Au) nanoparticles as a function of the metals volume ratio. Journal of Applied Physics, 2020, 128, .	2.5	7
39	Epitaxial Growth of a Gold Shell on Intermetallic FeRh Nanocrystals. Crystal Growth and Design, 2020, 20, 4144-4149.	3.0	7
40	Ferroelastic behaviour of the (Ln)Ba ₂ Cu ₃ O _{6+x} orthorhombic phase. Ferroelectrics, 1989, 97, 181-186.	0.6	4
41	Sputter growth and magnetic properties of exchange-biased La[sub 1/4]Ca[sub 3/4]MnO[sub 3]–La[sub 2/3]Sr[sub 1/3]MnO[sub 3] epitaxial bilayers. Journal of Applied Physics, 2002, 91, 7730.	2.5	4
42	Development of Bi-Metallic Fe—Bi Nanocomposites: Synthesis and Characterization. Journal of Nanoscience and Nanotechnology, 2012, 12, 8640-8646.	0.9	4
43	Visualising alloy fluctuations by spherical-aberration–corrected HRTEM. Europhysics Letters, 2010, 91, 36001.	2.0	2
44	Synthesis and Self-Assembly of Monodisperse Indium Nanoparticles Prepared from the Organometallic Precursor. Angewandte Chemie - International Edition, 2001, 40, 448-451.	13.8	2
45	Self-organization mecanisms in a Fe-Au film: from isolated core-shell to multicore nanoparticles. EPJ Applied Physics, 0, , .	0.7	2
46	Composition-structure correlations in strained Fe[sub x]Mn[sub 1â^'x]/Ir superlattices. Journal of Applied Physics, 2000, 88, 4605.	2.5	0
47	Microstructural Features of a-Axis Oriented YBa2Cu3O7-Î′/PrBa2Cu3O7-Î′/YBa2Cu3O7-ÎJunctions Studied by Transmission Electron Microscopy. Microscopy Microanalysis Microstructures, 1996, 7, 255-264.	0.4	Ο